Acta Cryst E CRYSTALLOGRAPHIC COMMUNICATIONS
ISSN 2056-9890

Crystal structure, Hirshfeld surface analysis and DFT studies of 1-[*r*-2,*c*-6-diphenyl-*t*-3-(propan-2-yl)piperidin-1-yl]ethan-1-one

P. Periyannan,[a] M. Beemarao,[a] K. Karthik,[b] S. Ponnuswamy[b] and K. Ravichandran[a]*

[a]Department of Physics, Kandaswami Kandar's College, Velur, Namakkal 638 182, India, and [b]PG and Research Department of Chemistry, Government Arts College (Autonomous), Coimbatore 641 018., Tamil Nadu, India. *Correspondence e-mail: kravichandran05@gmail.com

Received 9 December 2019
Accepted 12 February 2020

Edited by D. Chopra, Indian Institute of Science Education and Research Bhopal, India

Keywords: crystal structure; piperidine derivative; Hirshfeld surface; DFT.

CCDC reference: 1814839

Supporting information: this article has supporting information at journals.iucr.org/e

In the title compound, $C_{22}H_{27}NO$, the piperidine ring adopts a chair conformation. The dihedral angles between the mean plane of the piperidine ring and the phenyl rings are 89.78 (7) and 48.30 (8)°. In the crystal, molecules are linked into chains along the *b*-axis direction by C—H···O hydrogen bonds. The DFT/B3LYP/6–311 G(d,p) method was used to determine the HOMO–LUMO energy levels. The molecular electrostatic potential surfaces were investigated by Hirshfeld surface analysis and two-dimensional fingerprint plots were used to analyse the intermolecular interactions in the molecule.

1. Chemical context

Piperidine is a heterocyclic six-membered ring containing nitrogen as a hetero atom and is an essential structural part of many important drugs including paroxetine, raloxifene, haloperidol, droperidol and minoxidiln (Wagstaff *et al.*, 2002). Piperidine derivatives exhibit a wide range of biological activities, such as antimicrobial, anti-inflammatory, antiviral, antimalarial and general anesthetic (Aridoss *et al.*, 2009). The biological properties of piperidines are highly dependent on the type and position of substituents on the heterocyclic ring. 2,6-Disubstituted piperidine derivatives have been found to possess fungicidal, bactericidal and herbicidal activities (Mobio *et al.*, 1989). Piperidine derivatives are the intermediate products in agrochemicals, pharmaceuticals, rubber vulcanization accelerators and are widely used as building block molecules in many industries. Various piperidine derivatives are present in numerous alkaloids (Badorrey *et al.*, 1999).

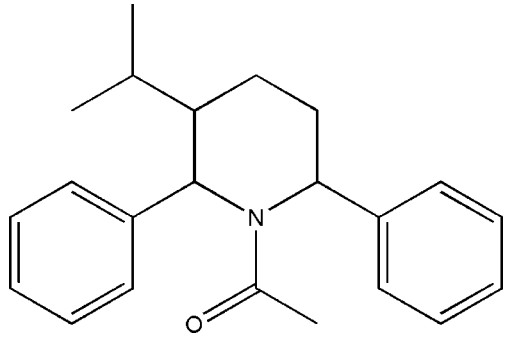

This wide range of biological activities prompted us to synthesize novel 2,6-diphenyl piperdine derivatives. Against this background, the structure of the title compound has been determined.

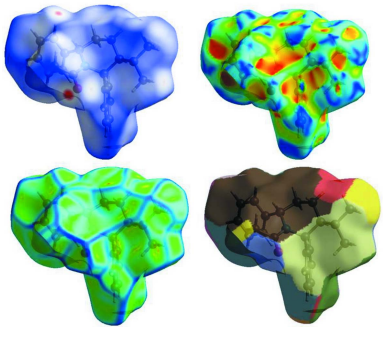

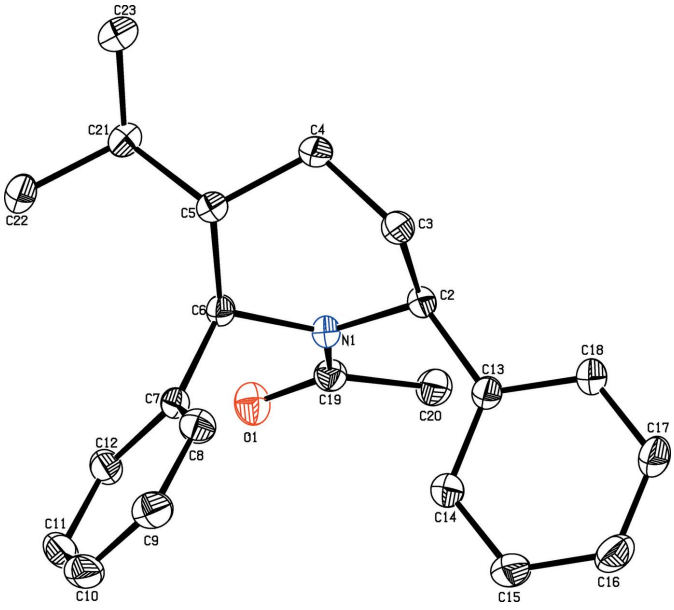

Figure 1
The molecular structure of the title compound, showing the atomic numbering and displacement ellipsoids drawn at the 30% probability level.

2. Structural commentary

The molecular structure of the title compound is shown in Fig. 1. The diphenyl-substituted piperidine compound crystallizes in the monoclinic space group $P2_1/n$. The bond lengths and angles are well within the expected limits and comparable with literature values (Allen *et al.*, 1998).

The piperidine ring adopts a chair conformation with the puckering parameters Q_2 = 0.6191 (15) Å and $\phi 2$ = 335.12 (14) Å. The piperidine ring (N1/C2–C6) makes dihedral angles of 89.78 (7) and 48.30 (8)°, respectively, with the C7–12 and C13–C18 phenyl rings, and confirms the fact that the moieties are in an axial orientations.

The keto and methyl groups substituted at atom C19 are equatorially orientated as confirmed from the torsion angle values O1—C19—N1—C2 = 177.54 (12)° and C20—C19—N1—C6 = 172.81 (11)°. In the molecule, the isopropyl group substituted at the 5-position of the piperidine ring is equatorially oriented, as confirmed by the torsion angles of C4—C5—C21—C22 = −172.13 (14)° and C6—C5—C21—C23 = −174.73 (14)°. The sum of the bond angles (359.87°) around atom N1 of the piperidine ring is in accordance with the sp^2-hybridization state (Beddoes *et al.*, 1986).

Table 1
Hydrogen-bond geometry (Å, °).

D—H···A	D—H	H···A	D···A	D—H···A
C9—H9···O1^{i}	0.93	2.54	3.4378 (19)	163

Symmetry code: (i) $x-\frac{1}{2}, -y+\frac{1}{2}, z-\frac{1}{2}$.

3. Supramolecular features

In the crystal, molecules are linked into $C(8)$ chains along the b-axis direction by C—H···O hydrogen bonds (Table 1, Fig. 2). The overall crystal packing of the title compound is shown in Fig. 3.

4. DFT study

The optimized structure of the molecule in the gas phase was generated theoretically *via* density functional theory (DFT) using standard B3LYP functional and 6-311G(d,p) basis-set

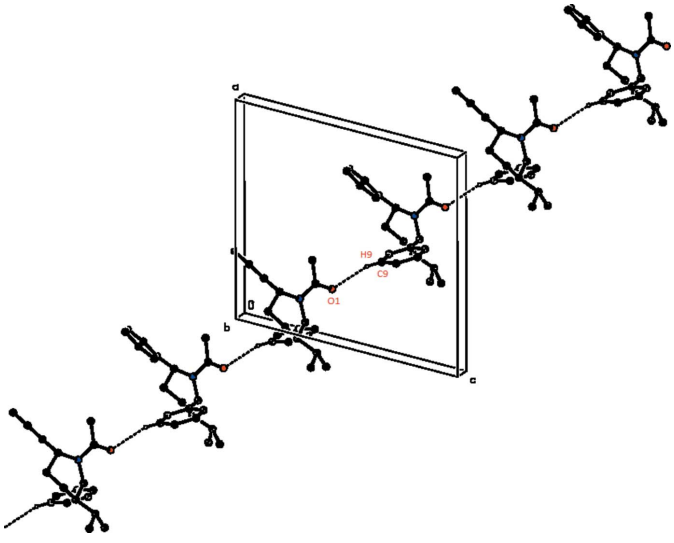

Figure 2
A partial view along the b axis of the crystal packing of the title compound, showing the formation of a molecular chain by C—H···O interactions (dotted lines).

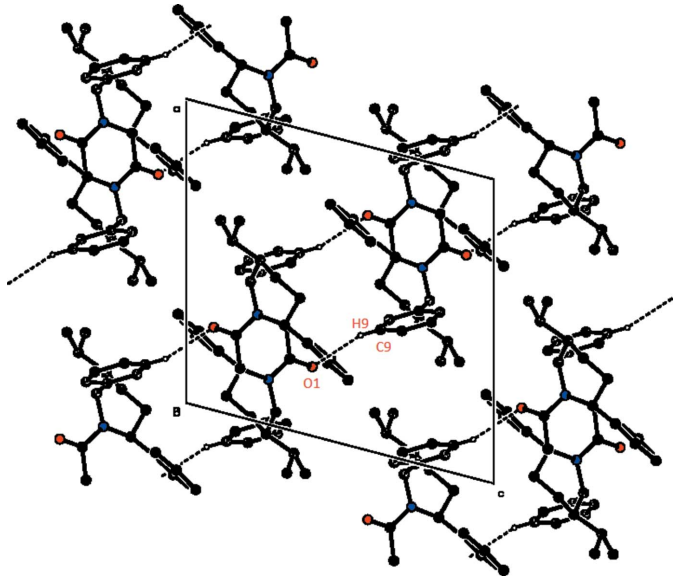

Figure 3
The overall crystal packing of the title compound, viewed along the b-axis direction. Hydrogen bonds are shown as dashed lines, and only the H atoms involved in hydrogen bonding have been included.

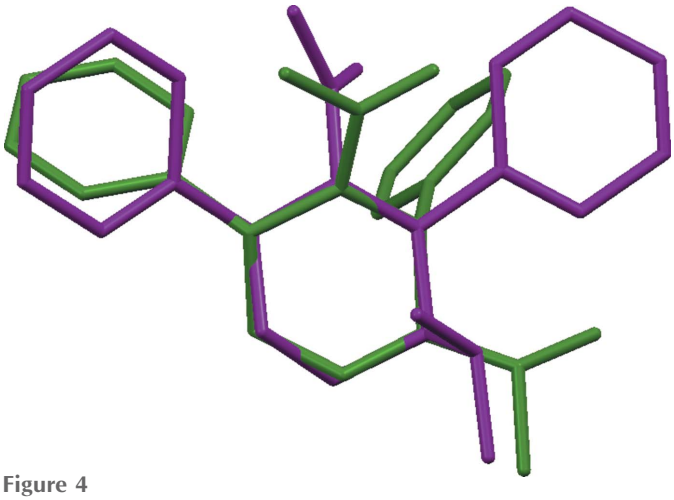

Figure 4
A structural overlay diagram (*Mercury*; Macrae *et al.*, 2020) for the optimized structure (purple) and the solid-state structure (green) of the title compound.

calculations (Becke *et al.*, 1993), as implemented in *GAUSSIAN09* (Frisch *et al.*, 2009).

The overlay diagram for the optimized structure (purple) and the structure in solid state (green) with respect to the piperidine ring is shown in Fig. 4. The piperidine rings in the two phases have an r.m.s deviation of 0.434 Å for the non-hydrogen atoms. The conformation of the molecules in the two phases differs with respect to the central piperidine ring, as seen in the disparity of about 38.5° in the N1—C6—C5—C4 torsion angles (39.88/1.38°) and 2.25° in the N1—C2—C3—C4 torsion angles (44.41/39.81°) for the optimized and solid-state molecules, respectively.

The highest-occupied molecular orbital (HOMO), acting as an electron donor, and the lowest-unoccupied molecular orbital (LUMO), acting as an electron acceptor, are known as

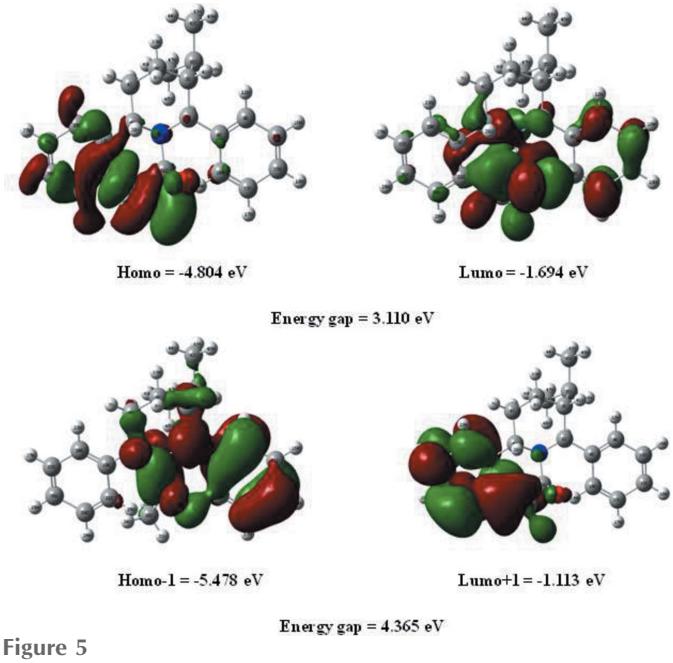

Figure 5
The frontier molecular orbitals (FMOs) of the title compound.

Table 2
Calculated frontier molecular orbital analysis of the title compound.

Parameter	Value
E_{HOMO} (eV)	−4.804
E_{LUMO} (eV)	−1.694
Energy gap, ΔE (eV)	3.110
HOMO−1 (eV)	−5.478
LUMO+1 (eV)	−1.113
Ionization potential, I (eV)	4.804
Electron affinity, A	1.694
Electrophilicity Index, ω	3.394
Hardness, η	1.555
Electro negativity, χ	3.249
Softness, σ	0.322

frontier molecular orbitals (FMOs). The FMOs play an important role in the optical and electric properties, as well as in quantum chemistry (Fleming, 1976). When the energy gap is small, the molecule is highly polarizable and has high chemical reactivity. The electron distribution of the HOMO−1, HOMO, LUMO and LUMO+1 energy levels and the energy values are shown in Fig. 5. The positive and negative phases are shown in green and red, respectively.

The HOMO of the title molecule is localized on the C═O group, one aromatic ring and the piperidine ring, while the LUMO is located over the whole molecule expect for the isopropyl group. The DFT study shows that the FMO energies E_{HOMO} and E_{LUMO} are −4.804 and −1.694 eV, respectively, and the HOMO–LUMO energy gap is 3.110 eV. The title compound has a small frontier orbital gap, hence the molecule has high chemical reactivity and low kinetic stability.

The electron affinity (I) and ionization potential (A) of the molecule were calculated using the DFT/B3LYP/6-311++G(d,p) basis set. A high value of the electrophilicity index describes a good electrophile, while a small value of electrophilicity index describes a good nucleophile. The values of the hardness (η), softness (σ), electronegativity (χ) and electrophilicity index (ω) for the title compound are given in Table 2.

5. Hirshfeld surface analysis

CrystalExplorer17 (Turner *et al.*, 2017) was used for the Hirshfeld surface (HS) analysis (Spackman & Jayatilaka, 2009) and to generate the associated two-dimensional fingerprint plots (McKinnon *et al.*, 2007) to quantify the various intermolecular interactions in the structure of the title compound. In the HS plotted over d_{norm} (Fig. 6), the white surface indicates contacts with distances equal to the sum of the van der Waals radii, and the red and blue colours indicate distances shorter (in close contact) or longer (distinct contact) than the van der Waals radii, respectively (Venkatesan *et al.*, 2016).

The HS mapped over curvedness and shape-index, introduced by Koendrink (Koenderink, 1990; Koenderink & van Doorn, 1992), give further chemical insight into molecular packing. A surface with low curvedness designates a flat region and may be indicative of π–π stacking in the crystal. A

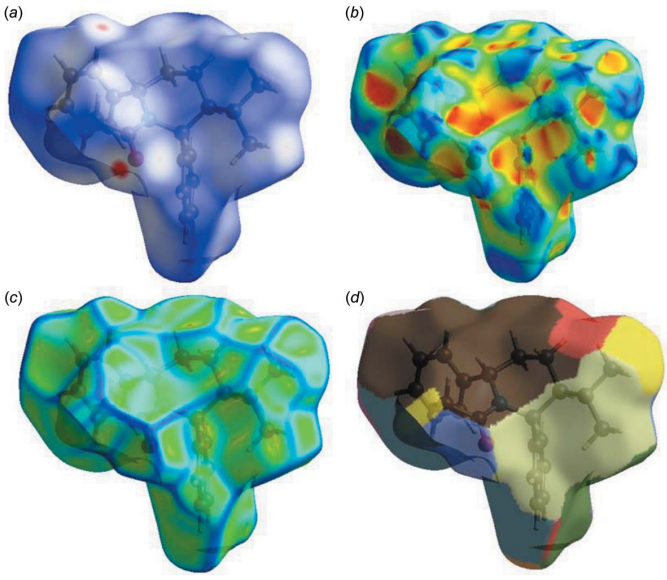

Figure 6
Hirshfeld surfaces mapped over (*a*) d_{norm}, (*b*) shape-index, (*c*) curvedness and (*d*) fragment patches.

Hirshfeld surface with high curvedness is highlighted as dark-blue edges, and is indicative of the absence of π–π stacking (Fig. 6). The nearest neighbour coordination environment of a molecule is identified from the colour patches on the Hirshfeld surface, depending on their closeness to adjacent molecules (Mohamooda Sumaya *et al.*, 2018).

The 2D fingerprint plots of the d_i and d_e points for the contacts contributing to the Hirshfeld surface are shown in Fig. 7. They indicate that intermolecular H···H contacts provide the largest contribution (74.2%) to the Hirshfeld surface. The percentage contributions of the other interactions are C···H/H···C = 18.7%, O···H/H···O = 7.0% and N···H/H···N = 0.1%. The Hirshfeld surface analysis confirms the importance of H-atom contacts in establishing the packing. The large number of H···H, H···C/C···H, H···O/O···H and H···N/N···H interactions suggest that hydrogen bonding and van der Waals interactions play the major roles in the crystal packing (Hathwar *et al.*, 2015).

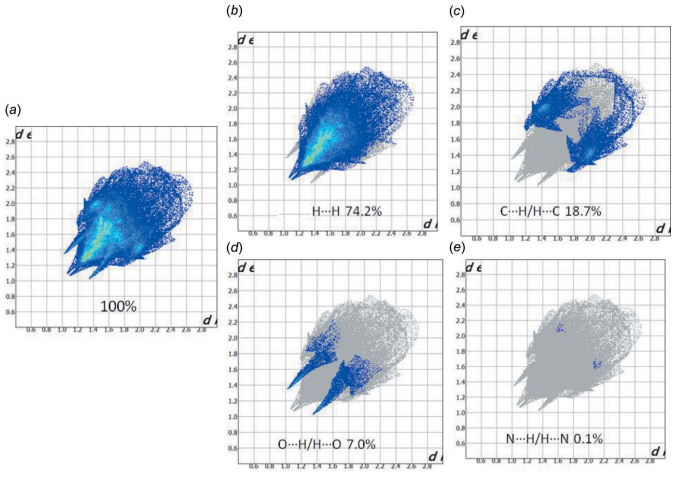

Figure 7
Two-dimensional fingerprint plot for the title compound showing the contributions of individual types of interactions: (*a*) all intermolecular contacts, (*b*) H···H contacts, (*c*) C···H/H···C contacts, (*d*) O···H/H···O contacts, (*e*) N···H/H···N contacts.

6. Database survey

A search of the Cambridge Structural Database (CSD, version 5.39; Groom *et al.*, 2016) using piperidine as the main skeleton revealed the presence of more than 30 records with different substituents on the piperidine ring. However, there are only two compounds with the same skeleton as the title compound, *viz.* *r*-2,*c*-6-diphenylpiperidine (NIKYEN; Maheshwaran *et al.*, 2013) and methyl 4-oxo-*r*-2,*c*-6-diphenylpiperidine-3-carboxylate (BIHZEY; Sampath *et al.*, 2004). In these compounds, the piperidine ring adopts a chair conformation as the title compound. The phenyl rings substituted at the 2- and 6-positions of the piperidine ring subtend dihedral angles of 89.78 (7) and 48.30 (8)°, respectively, with the best plane of the piperidine ring in the title compound and 81.04 (7) and 81.10 (7)°, respectively, in NIKYEN, whereas in BIHZEY they are equatorially oriented. The C—H···O interaction leads to the formation of a *C*(8) chain in the title compound, while it forms dimers in the other two structures.

7. Synthesis and crystallization

t-3-Isopropyl-*r*-2,*c*-6-diphenylpiperidin-4-one was reduced to the corresponding piperidine using the Wolf–Kishner reduction (Ravindran & Jeyaraman, 1992). Piperidine-4-one (10 mmol) was treated with diethylene glycol (40 ml), hydrazine hydrate (10 mmol) and KOH pellets (10 mmol) to give *t*-3-isopropyl-*r*-2,*c*-6-diphenylpiperidine. *N*-Acetyl piperidine was synthesized by the acetylation of the above piperidine. To *t*-3-isopropyl-*r*-2,*c*-6-diphenylpiperidine (5 mmol) dissolved in benzene (50 ml) were added triethylamine (20 mmol) and acetyl chloride (20 mmol) to give the title compound, which was crystallized by slow evaporation from a benzene/petroleum ether **(*v*:*v* = ?:?)** solution.

8. Refinement

Crystal data, data collection and structure refinement details are summarized in Table 3. H atoms were positioned geometrically (N—H = 0.88–0.90 Å and C—H = 0.93–0.98 Å) and allowed to ride on their parent atoms,with U_{iso}(H) = 1.5*U*eq(C) for methyl H 1.2*U*eq(C) for other H atoms.

Acknowledgements

The authors thank the SAIF, IIT Madras, India, for the data collection.

Funding information

KR thanks the UGC, New Delhi, for financial assistance in the form of a Minor Research Project.

Table 3
Experimental details.

Crystal data	
Chemical formula	$C_{22}H_{27}NO$
M_r	321.44
Crystal system, space group	Monoclinic, $P2_1/n$
Temperature (K)	296
a, b, c (Å)	13.3077 (5), 10.3009 (4), 13.9338 (5)
β (°)	104.657 (1)
V (Å^3)	1847.91 (12)
Z	4
Radiation type	Mo $K\alpha$
μ (mm^{-1})	0.07
Crystal size (mm)	0.30 × 0.25 × 0.20
Data collection	
Diffractometer	Bruker *SMART* APEXII CCD
Absorption correction	Multi-scan (*SADABS*; Bruker, 2008)
T_{min}, T_{max}	0.979, 0.986
No. of measured, independent and observed [$I > 2\sigma(I)$] reflections	43393, 5246, 3546
R_{int}	0.028
(sin $\theta/\lambda)_{max}$ (Å^{-1})	0.707
Refinement	
$R[F^2 > 2\sigma(F^2)]$, $wR(F^2)$, S	0.053, 0.169, 1.02
No. of reflections	5246
No. of parameters	221
H-atom treatment	H-atom parameters constrained
$\Delta\rho_{max}$, $\Delta\rho_{min}$ (e Å^{-3})	0.45, −0.22

Computer programs: *APEX2* and *SAINT*, *SHELXS97* and *SHELXL97* (Sheldrick, 2008), *SHELXL2018* (Sheldrick, 2015), *ORTEP-3 for Windows* (Farrugia, 2012) and *PLATON* (Spek, 2020).

References

Allen, F. H., Shields, G. P., Taylor, R., Allen, F. H., Raithby, P. R., Shields, G. P. & Taylor, R. (1998). *Chem. Commun.* pp. 1043–1044.
Aridoss, G., Parthiban, P., Ramachandran, R., Prakash, M., Kabilan, S. & Jeong, Y. T. (2009). *Eur. J. Med. Chem.* **44**, 577–592.
Badorrey, R., Cativiela, C., Díaz-de-Villegas, M. D. & Gálvez, J. A. (1999). *Tetrahedron*, **55**, 7601–7612.
Becke, A. (1993). *J. Chem. Phys.* **98**, 5648–5652.
Beddoes, R. L., Dalton, L., Joule, T. A., Mills, O. S., Street, J. D. & Watt, C. I. F. (1986). *J. Chem. Soc. Perkin Trans. 2*, pp. 787–797.
Bruker (2008). *APEX2*, *SAINT* and *SADABS*. Bruker AXS Inc., Madison, Wisconsin, USA.
Farrugia, L. J. (2012). *J. Appl. Cryst.* **45**, 849–854.
Fleming, I. (1976). *Frontier Orbitals and Organic Chemical Reactions.* London: Wiley.
Frisch, M. J., , *et al.* (2009). *GAUSSIAN09*. Gaussian Inc., Wallingford, CT, USA.
Groom, C. R., Bruno, I. J., Lightfoot, M. P. & Ward, S. C. (2016). *Acta Cryst.* B**72**, 171–179.
Hathwar, V. R., Sist, M., Jørgensen, M. R. V., Mamakhel, A. H., Wang, X., Hoffmann, C. M., Sugimoto, K., Overgaard, J. & Iversen, B. B. (2015). *IUCrJ*, **2**, 563–574.
Koenderink, J. J. (1990). *Solid Shape*. Cambridge MA: MIT Press.
Koenderink, J. J. & van Doorn, A. J. (1992). *Image Vis. Comput.* **10**, 557–564.
Macrae, C. F., Sovago, I., Cottrell, S. J., Galek, P. T. A., McCabe, P., Pidcock, E., Platings, M., Shields, G. P., Stevens, J. S., Towler, M. & Wood, P. A. (2020). *J. Appl. Cryst.* **53**, 226–235.
Maheshwaran, V., Abdul Basheer, S., Akila, A., Ponnuswamy, S. & Ponnuswamy, M. N. (2013). *Acta Cryst.* E**69**, o1371.
McKinnon, J. J., Jayatilaka, D. & Spackman, M. A. (2007). *Chem. Commun.* pp. 3814–3816.
Mobio, I. G., Soldatenkov, A. T., Federov, V. O., Ageev, E. A., Sergeeva, N. D., Lin, S., Stashenku, E. E., Prostakov, N. S. & Andreeva, E. L. (1989). *Khim. Farm. Zh.* **23**, 421–427.
Mohamooda Sumaya, U., Sankar, E., Arasambattu MohanaKrishnan, K., Biruntha, K. & Usha, G. (2018). *Acta Cryst.* E**74**, 878–883.
Ravindran, T. & Jeyaraman, R. (1992). *Indian J. Chem.* B**31**, 677–682.
Sampath, N., Aravindhan, S., Ponnuswamy, M. N. & Nethaji, M. (2004). *Acta Cryst.* E**60**, o2105–o2106.
Sheldrick, G. M. (2008). *Acta Cryst.* A**64**, 112–122.
Sheldrick, G. M. (2015). *Acta Cryst.* C**71**, 3–8.
Spackman, M. A. & Jayatilaka, D. (2009). *CrystEngComm*, **11**, 19–32.
Spek, A. L. (2020). *Acta Cryst.* E**76**, 1–11.
Turner, M. J., McKinnon, J. J., Wolff, S. K., Grimwood, D. J., Spackman, P. R., Jayatilaka, D. & Spackman, M. A. (2017). *CrystalExplorer17. University of Western Australia.* http://hirshfeldsurface.net.
Venkatesan, P., Thamotharan, S., Ilangovan, A., Liang, H. & Sundius, T. (2016). *Spectrochim. Acta*, A**153**, 625–636.
Wagstaff, A. J., Cheer, S. M., Matheson, A. J., Ormrod, D. & Goa, K. L. (2002). *Drugs*, **62**, 655–703.

supporting information

Acta Cryst. (2020). E**76**, 377-381 [https://doi.org/10.1107/S2056989020002042]

Crystal structure, Hirshfeld surface analysis and DFT studies of 1-[*r*-2,*c*-6-diphenyl-*t*-3-(propan-2-yl)piperidin-1-yl]ethan-1-one

P. Periyannan, M. Beemarao, K. Karthik, S. Ponnuswamy and K. Ravichandran

Computing details

Data collection: *APEX2* (Bruker, 2008); cell refinement: *SAINT* (Bruker, 2008); data reduction: *SAINT*; program(s) used to solve structure: *SHELXS97* (Sheldrick, 2008); program(s) used to refine structure: *SHELXL2018* (Sheldrick, 2015); molecular graphics: *ORTEP-3 for Windows* (Farrugia, 2012); software used to prepare material for publication: *SHELXL97* (Sheldrick, 2008) and *PLATON* (Spek, 2020).

N-acetyl-3-isopropyl-2,6-diphenylpiperidine

Crystal data

$C_{22}H_{27}NO$
$M_r = 321.44$
Monoclinic, $P2_1/n$
$a = 13.3077$ (5) Å
$b = 10.3009$ (4) Å
$c = 13.9338$ (5) Å
$\beta = 104.657$ (1)°
$V = 1847.91$ (12) Å^3
$Z = 4$
$F(000) = 696$
$D_x = 1.155$ Mg m^{-3}
Mo $K\alpha$ radiation, $\lambda = 0.71073$ Å
Cell parameters from 3546 reflections
$\theta = 1.9$–30.2°
$\mu = 0.07$ mm^{-1}
$T = 296$ K
Block, white crystalline
0.30 × 0.25 × 0.20 mm

Data collection

Bruker SMART APEXII CCD diffractometer
Radiation source: fine-focus sealed tube
ω and φ scans
Absorption correction: multi-scan (*SADABS*; Bruker, 2008)
$T_{min} = 0.979$, $T_{max} = 0.986$
43393 measured reflections
5246 independent reflections
3546 reflections with $I > 2\sigma(I)$
$R_{int} = 0.028$
$\theta_{max} = 30.2°$, $\theta_{min} = 1.9°$
$h = -18\rightarrow18$
$k = -14\rightarrow14$
$l = -19\rightarrow19$

Refinement

Refinement on F^2
Least-squares matrix: full
$R[F^2 > 2\sigma(F^2)] = 0.053$
$wR(F^2) = 0.169$
$S = 1.02$
5246 reflections
221 parameters
0 restraints
Hydrogen site location: inferred from neighbouring sites
H-atom parameters constrained
$w = 1/[\sigma^2(F_o^2) + (0.0897P)^2 + 0.2822P]$ where $P = (F_o^2 + 2F_c^2)/3$
$(\Delta/\sigma)_{max} = 0.001$
$\Delta\rho_{max} = 0.45$ e Å^{-3}
$\Delta\rho_{min} = -0.22$ e Å^{-3}
Extinction correction: SHELXL2018 (Sheldrick, 2015), $Fc^*=kFc[1+0.001xFc^2\lambda^3/\sin(2\theta)]^{-1/4}$
Extinction coefficient: 0.028 (3)

Special details

Geometry. All esds (except the esd in the dihedral angle between two l.s. planes) are estimated using the full covariance matrix. The cell esds are taken into account individually in the estimation of esds in distances, angles and torsion angles; correlations between esds in cell parameters are only used when they are defined by crystal symmetry. An approximate (isotropic) treatment of cell esds is used for estimating esds involving l.s. planes.

Fractional atomic coordinates and isotropic or equivalent isotropic displacement parameters (Å²)

	x	*y*	*z*	U_{iso}*/U_{eq}
C2	0.65890 (11)	−0.04974 (12)	0.67960 (9)	0.0430 (3)
H2	0.710803	−0.117590	0.703575	0.052*
C3	0.55791 (12)	−0.11907 (14)	0.63075 (11)	0.0535 (4)
H3A	0.509789	−0.058442	0.589793	0.064*
H3B	0.571443	−0.188289	0.588507	0.064*
C4	0.51045 (13)	−0.17493 (14)	0.70987 (12)	0.0553 (4)
H4A	0.562934	−0.221549	0.758707	0.066*
H4B	0.455515	−0.235360	0.680048	0.066*
C5	0.46657 (10)	−0.06466 (13)	0.75983 (10)	0.0434 (3)
H5	0.406942	−0.029180	0.710452	0.052*
C6	0.54640 (9)	0.04763 (12)	0.79099 (9)	0.0386 (3)
H6	0.561919	0.050544	0.863560	0.046*
C7	0.50324 (9)	0.18152 (12)	0.75655 (9)	0.0401 (3)
C8	0.44865 (11)	0.20754 (15)	0.65996 (11)	0.0509 (3)
H8	0.438587	0.141664	0.612841	0.061*
C9	0.40861 (12)	0.33048 (16)	0.63217 (13)	0.0608 (4)
H9	0.372408	0.346381	0.566876	0.073*
C10	0.42249 (12)	0.42814 (15)	0.70093 (15)	0.0649 (5)
H10	0.395238	0.510190	0.682456	0.078*
C11	0.47650 (13)	0.40503 (15)	0.79693 (15)	0.0639 (4)
H11	0.486050	0.471484	0.843544	0.077*
C12	0.51698 (11)	0.28257 (14)	0.82473 (11)	0.0508 (3)
H12	0.553878	0.267904	0.889987	0.061*
C13	0.69896 (10)	0.03120 (13)	0.60592 (9)	0.0435 (3)
C14	0.68956 (14)	0.16488 (15)	0.59909 (12)	0.0593 (4)
H14	0.656620	0.209142	0.640704	0.071*
C15	0.72856 (16)	0.23353 (17)	0.53114 (13)	0.0693 (5)
H15	0.722127	0.323421	0.527699	0.083*
C16	0.77685 (15)	0.16916 (19)	0.46859 (13)	0.0695 (5)
H16	0.803555	0.215281	0.423235	0.083*
C17	0.78528 (15)	0.03651 (18)	0.47370 (13)	0.0664 (5)
H17	0.816965	−0.007417	0.430922	0.080*
C18	0.74709 (12)	−0.03242 (15)	0.54185 (11)	0.0528 (4)
H18	0.753688	−0.122304	0.544822	0.063*
C19	0.73417 (10)	0.06355 (13)	0.83744 (10)	0.0443 (3)
C20	0.83981 (11)	0.02750 (16)	0.82495 (13)	0.0565 (4)
H20A	0.851320	0.070404	0.767506	0.085*
H20B	0.843344	−0.064779	0.816729	0.085*
H20C	0.892096	0.053889	0.882667	0.085*

C21	0.42650 (12)	−0.10889 (15)	0.84920 (12)	0.0546 (4)
H21	0.486985	−0.132684	0.902717	0.065*
C22	0.37021 (14)	0.00100 (17)	0.88713 (14)	0.0665 (5)
H22A	0.313140	0.030351	0.834665	0.100*
H22B	0.417520	0.071598	0.909149	0.100*
H22C	0.344502	−0.029708	0.941477	0.100*
C23	0.35598 (17)	−0.22597 (19)	0.82723 (17)	0.0826 (6)
H23A	0.299342	−0.208302	0.770673	0.124*
H23B	0.329279	−0.244610	0.883608	0.124*
H23C	0.394522	−0.299376	0.813439	0.124*
N1	0.64819 (8)	0.02265 (10)	0.76798 (7)	0.0396 (2)
O1	0.72737 (8)	0.12759 (12)	0.90987 (7)	0.0591 (3)

Atomic displacement parameters (Å²)

	U^{11}	U^{22}	U^{33}	U^{12}	U^{13}	U^{23}
C2	0.0512 (7)	0.0375 (6)	0.0451 (7)	0.0024 (5)	0.0209 (6)	−0.0028 (5)
C3	0.0679 (9)	0.0462 (7)	0.0528 (8)	−0.0114 (7)	0.0272 (7)	−0.0134 (6)
C4	0.0683 (9)	0.0406 (7)	0.0652 (9)	−0.0110 (6)	0.0322 (7)	−0.0093 (6)
C5	0.0452 (7)	0.0406 (6)	0.0475 (7)	−0.0036 (5)	0.0172 (5)	−0.0013 (5)
C6	0.0403 (6)	0.0406 (6)	0.0370 (6)	−0.0001 (5)	0.0135 (5)	−0.0022 (5)
C7	0.0361 (6)	0.0390 (6)	0.0482 (7)	−0.0005 (5)	0.0159 (5)	−0.0026 (5)
C8	0.0510 (8)	0.0485 (7)	0.0519 (8)	0.0004 (6)	0.0102 (6)	0.0004 (6)
C9	0.0479 (8)	0.0585 (9)	0.0731 (10)	0.0054 (7)	0.0097 (7)	0.0153 (8)
C10	0.0458 (8)	0.0446 (8)	0.1057 (14)	0.0073 (6)	0.0220 (9)	0.0102 (8)
C11	0.0551 (9)	0.0444 (8)	0.0961 (13)	0.0018 (6)	0.0264 (8)	−0.0164 (8)
C12	0.0490 (8)	0.0469 (7)	0.0585 (8)	−0.0001 (6)	0.0171 (6)	−0.0094 (6)
C13	0.0444 (7)	0.0455 (7)	0.0436 (7)	−0.0016 (5)	0.0166 (5)	−0.0024 (5)
C14	0.0767 (10)	0.0461 (8)	0.0656 (9)	0.0005 (7)	0.0375 (8)	0.0000 (7)
C15	0.0948 (13)	0.0505 (9)	0.0723 (10)	−0.0069 (8)	0.0390 (9)	0.0065 (8)
C16	0.0826 (12)	0.0743 (11)	0.0609 (9)	−0.0179 (9)	0.0357 (9)	0.0030 (8)
C17	0.0757 (11)	0.0735 (11)	0.0628 (9)	−0.0068 (9)	0.0411 (8)	−0.0087 (8)
C18	0.0575 (8)	0.0527 (8)	0.0548 (8)	0.0004 (6)	0.0264 (7)	−0.0062 (6)
C19	0.0435 (7)	0.0426 (7)	0.0472 (7)	0.0009 (5)	0.0122 (5)	0.0026 (5)
C20	0.0419 (7)	0.0572 (9)	0.0714 (10)	0.0005 (6)	0.0162 (7)	0.0017 (7)
C21	0.0575 (8)	0.0525 (8)	0.0612 (8)	−0.0021 (6)	0.0287 (7)	0.0055 (6)
C22	0.0701 (10)	0.0686 (10)	0.0743 (10)	−0.0087 (8)	0.0433 (9)	−0.0094 (8)
C23	0.0985 (15)	0.0604 (11)	0.1080 (15)	−0.0175 (10)	0.0617 (12)	−0.0009 (10)
N1	0.0411 (5)	0.0404 (5)	0.0398 (5)	0.0016 (4)	0.0149 (4)	−0.0026 (4)
O1	0.0509 (6)	0.0719 (7)	0.0518 (6)	−0.0013 (5)	0.0080 (4)	−0.0156 (5)

Geometric parameters (Å, º)

C2—N1	1.4770 (15)	C13—C14	1.384 (2)
C2—C13	1.5199 (18)	C13—C18	1.3878 (18)
C2—C3	1.522 (2)	C14—C15	1.384 (2)
C2—H2	0.9800	C14—H14	0.9300
C3—C4	1.516 (2)	C15—C16	1.377 (3)

C3—H3A	0.9700	C15—H15	0.9300
C3—H3B	0.9700	C16—C17	1.371 (3)
C4—C5	1.5238 (19)	C16—H16	0.9300
C4—H4A	0.9700	C17—C18	1.381 (2)
C4—H4B	0.9700	C17—H17	0.9300
C5—C21	1.5422 (19)	C18—H18	0.9300
C5—C6	1.5561 (18)	C19—O1	1.2280 (16)
C5—H5	0.9800	C19—N1	1.3648 (17)
C6—N1	1.4913 (15)	C19—C20	1.5061 (19)
C6—C7	1.5241 (17)	C20—H20A	0.9600
C6—H6	0.9800	C20—H20B	0.9600
C7—C8	1.3843 (19)	C20—H20C	0.9600
C7—C12	1.3897 (18)	C21—C23	1.511 (2)
C8—C9	1.390 (2)	C21—C22	1.524 (2)
C8—H8	0.9300	C21—H21	0.9800
C9—C10	1.369 (2)	C22—H22A	0.9600
C9—H9	0.9300	C22—H22B	0.9600
C10—C11	1.370 (3)	C22—H22C	0.9600
C10—H10	0.9300	C23—H23A	0.9600
C11—C12	1.388 (2)	C23—H23B	0.9600
C11—H11	0.9300	C23—H23C	0.9600
C12—H12	0.9300		

N1—C2—C13	114.24 (10)	C14—C13—C18	118.30 (13)
N1—C2—C3	110.44 (10)	C14—C13—C2	123.46 (12)
C13—C2—C3	112.10 (11)	C18—C13—C2	118.25 (12)
N1—C2—H2	106.5	C15—C14—C13	120.84 (15)
C13—C2—H2	106.5	C15—C14—H14	119.6
C3—C2—H2	106.5	C13—C14—H14	119.6
C4—C3—C2	109.64 (12)	C16—C15—C14	120.20 (16)
C4—C3—H3A	109.7	C16—C15—H15	119.9
C2—C3—H3A	109.7	C14—C15—H15	119.9
C4—C3—H3B	109.7	C17—C16—C15	119.48 (15)
C2—C3—H3B	109.7	C17—C16—H16	120.3
H3A—C3—H3B	108.2	C15—C16—H16	120.3
C3—C4—C5	109.13 (11)	C16—C17—C18	120.55 (15)
C3—C4—H4A	109.9	C16—C17—H17	119.7
C5—C4—H4A	109.9	C18—C17—H17	119.7
C3—C4—H4B	109.9	C17—C18—C13	120.63 (15)
C5—C4—H4B	109.9	C17—C18—H18	119.7
H4A—C4—H4B	108.3	C13—C18—H18	119.7
C4—C5—C21	113.54 (11)	O1—C19—N1	121.72 (12)
C4—C5—C6	111.60 (11)	O1—C19—C20	119.50 (13)
C21—C5—C6	110.21 (11)	N1—C19—C20	118.78 (12)
C4—C5—H5	107.0	C19—C20—H20A	109.5
C21—C5—H5	107.0	C19—C20—H20B	109.5
C6—C5—H5	107.0	H20A—C20—H20B	109.5
N1—C6—C7	112.27 (10)	C19—C20—H20C	109.5

N1—C6—C5	113.89 (10)	H20A—C20—H20C	109.5
C7—C6—C5	114.11 (10)	H20B—C20—H20C	109.5
N1—C6—H6	105.2	C23—C21—C22	109.18 (14)
C7—C6—H6	105.2	C23—C21—C5	113.34 (13)
C5—C6—H6	105.2	C22—C21—C5	111.18 (13)
C8—C7—C12	117.74 (13)	C23—C21—H21	107.6
C8—C7—C6	122.99 (12)	C22—C21—H21	107.6
C12—C7—C6	119.25 (12)	C5—C21—H21	107.6
C7—C8—C9	121.13 (14)	C21—C22—H22A	109.5
C7—C8—H8	119.4	C21—C22—H22B	109.5
C9—C8—H8	119.4	H22A—C22—H22B	109.5
C10—C9—C8	120.00 (15)	C21—C22—H22C	109.5
C10—C9—H9	120.0	H22A—C22—H22C	109.5
C8—C9—H9	120.0	H22B—C22—H22C	109.5
C9—C10—C11	120.01 (15)	C21—C23—H23A	109.5
C9—C10—H10	120.0	C21—C23—H23B	109.5
C11—C10—H10	120.0	H23A—C23—H23B	109.5
C10—C11—C12	120.09 (15)	C21—C23—H23C	109.5
C10—C11—H11	120.0	H23A—C23—H23C	109.5
C12—C11—H11	120.0	H23B—C23—H23C	109.5
C11—C12—C7	121.02 (15)	C19—N1—C2	120.44 (11)
C11—C12—H12	119.5	C19—N1—C6	116.00 (10)
C7—C12—H12	119.5	C2—N1—C6	123.43 (10)

N1—C2—C3—C4	−39.81 (16)	C18—C13—C14—C15	−1.0 (3)
C13—C2—C3—C4	−168.43 (12)	C2—C13—C14—C15	179.32 (15)
C2—C3—C4—C5	72.53 (16)	C13—C14—C15—C16	0.5 (3)
C3—C4—C5—C21	−173.93 (13)	C14—C15—C16—C17	0.5 (3)
C3—C4—C5—C6	−48.63 (16)	C15—C16—C17—C18	−0.9 (3)
C4—C5—C6—N1	−1.38 (15)	C16—C17—C18—C13	0.4 (3)
C21—C5—C6—N1	125.74 (12)	C14—C13—C18—C17	0.5 (2)
C4—C5—C6—C7	129.33 (12)	C2—C13—C18—C17	−179.74 (14)
C21—C5—C6—C7	−103.55 (13)	C4—C5—C21—C23	−48.70 (19)
N1—C6—C7—C8	82.58 (15)	C6—C5—C21—C23	−174.73 (14)
C5—C6—C7—C8	−48.92 (16)	C4—C5—C21—C22	−172.13 (14)
N1—C6—C7—C12	−98.65 (13)	C6—C5—C21—C22	61.84 (16)
C5—C6—C7—C12	129.85 (12)	O1—C19—N1—C2	177.54 (12)
C12—C7—C8—C9	−0.2 (2)	C20—C19—N1—C2	−3.16 (18)
C6—C7—C8—C9	178.56 (13)	O1—C19—N1—C6	−6.49 (18)
C7—C8—C9—C10	−0.3 (2)	C20—C19—N1—C6	172.81 (11)
C8—C9—C10—C11	0.5 (3)	C13—C2—N1—C19	−69.70 (15)
C9—C10—C11—C12	−0.2 (2)	C3—C2—N1—C19	162.84 (12)
C10—C11—C12—C7	−0.4 (2)	C13—C2—N1—C6	114.64 (13)
C8—C7—C12—C11	0.6 (2)	C3—C2—N1—C6	−12.81 (17)
C6—C7—C12—C11	−178.28 (13)	C7—C6—N1—C19	87.19 (13)
N1—C2—C13—C14	−23.54 (19)	C5—C6—N1—C19	−141.19 (11)
C3—C2—C13—C14	103.05 (16)	C7—C6—N1—C2	−96.97 (13)
N1—C2—C13—C18	156.75 (12)	C5—C6—N1—C2	34.64 (15)

C3—C2—C13—C18	−76.66 (16)

Hydrogen-bond geometry (Å, º)

D—H···*A*	*D*—H	H···*A*	*D*···*A*	*D*—H···*A*
C9—H9···O1^{i}	0.93	2.54	3.4378 (19)	163

Symmetry code: (i) *x*−1/2, −*y*+1/2, *z*−1/2.